J. Fluid Mech. (2005), *vol.* 524, *pp.* 207–228. © 2005 Cambridge University Press
DOI: 10.1017/S0022112004002356 Printed in the United Kingdom

Wave scattering in a two-layer fluid of varying depth

By P. G. CHAMBERLAIN AND D. PORTER

Department of Mathematics, University of Reading, P.O. Box 220, Whiteknights, Reading RG6 6AX, UK

(Received 16 December 2003 and in revised form 2 September 2004)

The scattering of waves in a two-layer fluid of varying mean depth is examined in a three-dimensional context using linear theory. A variational technique is used to construct a particular type of approximation which has the effect of removing the vertical coordinate and reducing the problem to two coupled partial differential equations in two independent variables. A transformation of this differential equation system leads to a particularly simple approximate representation of the scattering process. The theory is applied to two-dimensional scattering, for which a set of symmetry relations is derived. A selection of numerical results is presented to illustrate the principle interest in the problem, namely the energy transfer between surface and interfacial waves induced by bed undulations.

1. Introduction

Wave scattering and generation for free-surface motions in continuously stratified and multi-layered fluids has recently attracted a good deal of attention. One aspect that has been at the focus of many investigations is the transfer of energy from surface to internal waves.

Barthélemy, Kabbaj & Germain (2000) have considered the scattering of long surface waves by a vertical step in a two-layer fluid as a way of modelling the effect of a continental shelf on tides and with the aim of estimating the energy leakage into the interfacial mode. They overcame the invalidity of the shallow-water approximation at the step by introducing evanescent modes. The vertical step problem for a two-layer flow was first investigated in the context of shallow-water theory by Kelly (1969), who showed that the approximation is applicable only if $K/\gamma \ll 1$. Here $K = \sigma^2 h/g$, where h represents the overall fluid depth and σ the applied frequency, and $1-\gamma = \rho_1/\rho_2 < 1$ is the ratio of the fluid densities in the two layers. As the long-wave assumption implies that $K \ll 1$, the limitation derived by Kelly is extremely restrictive in applications where $\gamma \ll 1$, which is the case for realistic ocean values. Kelly (1969) therefore adopted an alternative approach by applying the variational plane wave approximation of Miles (1967) to a full linear formulation of the problem.

Lynett & Liu (2002) have also used a full formulation, but including weak nonlinearities, to investigate interfacial waves in a two-layer model with a small relative density difference. Variations in the bedform are incorporated by averaging over the fluid depth and the authors consider, in particular, scattering by a smooth shelf linking two horizontal bed sections. Chen & Liu (1996) consider the evolution of fully nonlinear waves over slowly varying random topography in a two-layer model, by transforming the governing equations into the modified Korteweg–de Vries equation.

https://doi.org/10.1017/S0022112004002356 Published online by Cambridge University Press

In contrast to these investigations, Llewellyn Smith & Young (2003) have recently obtained an analytic solution for the conversion of tidal energy into an internal wave by a steep ridge, modelled as a vertical barrier. They allow for continuous stratification and, by approximating the vertical eigenfunctions over a horizontal bed by means of the WKB method, reduce the problem to a weakly singular integral equation having an explicit solution in the case of uniform stratification. A numerical solution is implemented for non-uniform stratifications. It is shown that the energy conversion rate depends strongly on the stratification, although the model overestimates this rate.

A different aspect of scattering in a fluid of non-uniform density is typified by the investigation of Linton & McIver (1995). Using linear theory, they examined the interaction of surface and interfacial waves with a horizontal circular cylinder, motivated in part by the application to a submerged pipe bridge across a fjord, which is well-approximated by the two-layer model used. This work is extended in Cadby & Linton (2000) and Linton & Cadby (2002), where references may be found to other investigations involving wave–structure interactions.

In the present paper we also use linear theory and we examine the three-dimensional problem of wave scattering in a two-layer fluid by arbitrary, slowly varying topography. Our aim is to derive a simple approximation to estimate the scattering process and, in particular, the way in which a varying bedform induces energy transfer between the two propagating modes that exist. Although our approach differs from those cited earlier, it has something in common with several of them in that it involves an approximation that is based on a slowly modulating wave function and it averages the motion over the depth.

The approximation is constructed by means of a variational principle, in effect Hamilton's principle, that is equivalent to the equations describing the problem. Solving these equations is thus equivalent to locating the stationary point of the governing functional. The Rayleigh–Ritz approximation may therefore be invoked: that an approximation to the stationary point of the functional is also an approximate solution of the equations. The principle may be used to determine this solution arbitrarily closely, by using the Rayleigh–Ritz method with a large enough basis. Here, as we seek a simple model of the scattering process, we merely use a two-term approximation based on the propagating wave modes over a flat, horizontal bed on the assumption that the bedform is slowly varying. Because this approach prescribes the vertical structure of the motion, the vertical coordinate is removed when the variational principle is applied, reducing the problem to a pair of coupled partial differential equations in the two horizontal variables; the variations in the fluid depth appear in the coefficients of these equations.

The resulting coupled equation system is the counterpart in the two-layer model of the mild-slope equation, devised originally by Berkhoff (1973, 1976) and independently by Smith & Sprinks (1975), that approximates scattering in a single fluid over undulating beds. However, the equations that we derive are extensions of the more recent modified mild-slope equation, derived by Chamberlain & Porter (1995), in which previously neglected curvature terms are shown to be significant. An investigation by Porter (2003) resulted in a reduced form of the modified mild-slope equation and the corresponding analysis in the present problem also has a significant simplifying effect.

The approach, of prescribing the vertical component of the motion and removing it by integration, is reminiscent of shallow-water theory. In fact, the mild-slope approximation that we use is a generalization of the shallow-water approximation, having the advantage that it applies to all wavelengths.

https://doi.org/10.1017/S0022112004002356 Published online by Cambridge University Press

To illustrate the theory, we examine scattering by a number of bedforms in a two-dimensional context, which the approximation reduces to solving a pair of coupled ordinary differential equations. In fact we have three pairs of equations to compare at this point. One is obtained directly from the approximation method and a second is just a transformed version of it; solving both serves as a check on the computations. The third pair is a simplified form of the transformed system and the interest lies in the error incurred in making the simplification. A set of symmetry relations is derived between the sixteen scattering coefficients that arise in this problem, generalizing those given by Linton & McIver (1995) for the case in which the lower fluid is of infinite extent. A subset of these relations provides a further check on the numerical solution technique.

The plan of the paper is as follows. In § 2 we formulate the problem and identify the variational principle, which is used to derive the approximation in § 3. The application to two-dimensional scattering, including the symmetry relations and a selection of numerical results, is given in § 4.

2. Formulation

We use Cartesian coordinates with the x- and y-axes lying in the mean free surface $z=0$, where z is directed vertically upwards. The bed is given by $z=-h(x,y)$, $h(x,y)$ being a given, continuous function with piecewise continuous first derivatives. The upper fluid has density ρ^+ and the lower fluid density $\rho^->\rho^+$, the two meeting at an interface whose mean position is at $z=-d$.

The usual assumptions of linearized theory and the removal of the harmonic time dependence $\exp(-\mathrm{i}\sigma t)$ lead to equations for the time-independent velocity potential $\phi(x,y,z)$ that may be deduced from Wehausen & Laitone (1960), namely,

$$\left.\begin{aligned}
&\nabla^2\phi=0 \quad (z\in(-h,-d)\cup(-d,0)),\\
&\phi_z-K\phi=0 \quad (z=0),\\
&\phi_z^+=\phi_z^-, \quad \rho^+(\phi_z^+-K\phi^+)=\rho^-(\phi_z^--K\phi^-) \quad (z=-d),\\
&\phi_z+\nabla_h h\cdot\nabla\phi=0 \quad (z=-h),
\end{aligned}\right\} \tag{2.1}$$

holding for $-\infty<x,y<\infty$, where $K=\sigma^2/g$ and we have used the notation $\nabla_h=(\partial/\partial x,\partial/\partial y,0)$. The superscripts $\pm$ attached to ϕ and other functions refer to the upper $(+)$ and lower $(-)$ fluids but will only be used for their values at the interface. Other conditions, to be applied as $x^2+y^2\to\infty$, do not concern us at this stage.

The free-surface elevation is given by $\mathrm{Re}\{\zeta_f(x,y)\mathrm{e}^{-\mathrm{i}\sigma t}\}$ and the interfacial elevation by $\mathrm{Re}\{\zeta_i(x,y)\mathrm{e}^{-\mathrm{i}\sigma t}\}$, where

$$\zeta_f(x,y)=\mathrm{i}\sigma(\phi)_{z=0}/g, \quad \zeta_i(x,y)=\mathrm{i}\sigma(\phi_z^\pm)_{z=-d}/gK. \tag{2.2}$$

The starting point for generating approximations to the solution of the set of equations (2.1) is the functional

$$L(\psi)=\iint_{\mathscr{D}}\mathscr{L}\,\mathrm{d}x\,\mathrm{d}y,$$

where $\mathscr{D}$ denotes a simply connected domain in the plane $z=0$ with boundary $\mathscr{C}$ and

https://doi.org/10.1017/S0022112004002356 Published online by Cambridge University Press

the Lagrangian density is given by

$$\mathscr{L}(\psi, \nabla\psi) = \rho^+ \int_{-d}^{0} \nabla\psi \cdot \overline{\nabla\psi}\, \mathrm{d}z + \rho^- \int_{-h}^{-d} \nabla\psi \cdot \overline{\nabla\psi}\, \mathrm{d}z - K\rho^+ |\psi|^2_{z=0} - K \frac{|\rho^-\psi^- - \rho^+\psi^+|^2_{z=-d}}{(\rho^- - \rho^+)}. \quad (2.3)$$

This has the form $\mathscr{L} = \mathscr{T} - \mathscr{V}$, and it can be verified that $\frac{1}{4}\mathscr{T}$ and $\frac{1}{4}\mathscr{V}$ are respectively the kinetic energy and potential energy of the vertical filament of fluid at (x, y), averaged over a period $2\pi/\sigma$; the factor $1/4$ has been omitted from $\mathscr{L}$ for algebraic convenience. With $\rho^+ = \rho^-$ and the interfacial discontinuity discarded, the functional L is proportional to that used by Chamberlain & Porter (1995). It is an extension to a two-layer fluid, in the time-harmonic case and for linearized motions, of the general functional given by Luke (1967).

As expected from the Hamiltonian structure of L, the natural conditions of the variational principle $\delta L = 0$ are the governing equations of the motion. More precisely, if we consider variations $\delta\psi$ that vanish on the lateral boundary $\mathscr{C} \times [-h, 0]$, we find that L is stationary at $\psi = \phi$ if and only if ϕ satisfies the set of conditions (2.1). Thus we can determine an approximation to ϕ by choosing an appropriate finite-dimensional form of ψ and optimize it by enforcing $\delta L = 0$.

It will be convenient to use an inner product for brevity and the natural choice, suggested by (2.3), is

$$(u, v) = \rho^+ \int_{-d}^{0} u\overline{v}\, \mathrm{d}z + \rho^- \int_{-h}^{-d} u\overline{v}\, \mathrm{d}z, \quad (u, u) = ||u||^2. \quad (2.4)$$

Scaling the dependent variables in the upper and lower fluids by $(\rho^+)^{1/2}$ and $(\rho^-)^{1/2}$, respectively, allows the usual inner product for $L_2(-h, 0)$ to be used but, although this step has algebraic merit, it obscures the physical quantities.

The simplest approximation $\psi \approx \phi$ that can be used is based on the propagating plane wave modes over a flat bed. To identify these we set $\phi(x, y, z) = \chi(x, y)Z(h, z)$ in (2.1) giving $(\nabla^2 + \mu)\chi = 0$ together with the eigenvalue problem

$$\left.\begin{aligned} &Z'' - \mu Z = 0 \quad (z \in (-h, -d) \cup (-d, 0)), \\ &Z' - KZ = 0 \quad (z = 0), \quad Z' = 0 \quad (z = -h), \\ &Z^{+'} = Z^{-'}, \quad \rho^+(Z^{+'} - KZ^+) = \rho^-(Z^{-'} - KZ^-) \quad (z = -d), \end{aligned}\right\} \quad (2.5)$$

in which μ is the separation constant and, for the present purpose, h is a constant. Writing $\mathsf{L}Z \equiv Z''$, it follows easily that $(\mathsf{L}Z, W) = (Z, \mathsf{L}W)$ so that L is self-adjoint. Therefore the eigenvalues μ_i of the boundary value problem (2.5) are real and the eigenfunctions Z_i are orthogonal with respect to the inner product (2.4).

A direct solution of (2.5) with $\mu = k^2$ shows that

$$Z(h, z) = \begin{cases} \alpha\{k\cosh(kz) + K\sinh(kz)\} & (-d < z \leqslant 0), \\ \beta\cosh k(z + h) & (-h \leqslant z \leqslant -d), \end{cases} \quad (2.6)$$

where

$$\alpha = \alpha(h) = \frac{\rho K \sinh k(h - d)}{k\sinh(kh)\{K\cosh(kd) - k\sinh(kd)\}}, \quad \beta = \beta(h) = \frac{\rho K}{k\sinh(kh)}, \quad (2.7)$$

with $\rho = \rho^+/\rho^-$. The wavenumber k satisfies

$$\rho(k^2 - K^2) = \{K\coth(kd) - k\}\{K\coth k(h - d) - k\}. \quad (2.8)$$

https://doi.org/10.1017/S0022112004002356 Published online by Cambridge University Press

The dependence of α and β on the depth has been made explicit in preparation for the case in which h varies.

As is well-known (see, for example, Wehausen & Laitone 1960), there are two real, positive roots, k_1 and k_2 say, of (2.8) for each ρ and K and these give rise to propagating wave modes through $(\nabla^2 + k_i^2)\chi = 0$. There is also an infinity of negative eigenvalues μ_i of (2.5) and these correspond to evanescent wave modes that do not concern us here. The relevant roots of (2.8) are ordered so that $k_1 < k_2$ and Z, α and β are accordingly written Z_i, α_i and β_i with $i = 1, 2$ to distinguish the two modes.

The eigenfunctions Z_i are, of course, arbitrary to within constant multipliers and the form of (2.6) has been chosen to ensure that it has appropriate behaviour in the single-layer limits. For small values of $1-\rho$, we find that $k_1 = k_0 + O(1-\rho)$, where k_0 is the positive real root of the single-layer dispersion relation $K = k\tanh(kh)$, and $k_2 \sim 2K/(1-\rho)$. Also, as $h-d \to 0$ with ρ and d fixed, $k_1 \to k_0$ and $k_2 \sim \{K/(1-\rho)(h-d)\}^{1/2} \to \infty$ and, since d and $h-d$ are interchangeable in the dispersion relation (2.8), we infer that $k_1 \to k_0$ and $k_2 \sim \{K/(1-\rho)d\}^{1/2} \to \infty$ as $d \to 0$ with ρ and h fixed.

Using this information in (2.6) it can be shown that in each of the limiting cases $Z_1(h, z) \to Z_0(h, z) = \rho\,\mathrm{sech}(kh)\cosh k(z+h)$ and $Z_2 \to 0$ for $-h \leqslant z \leqslant 0$, where Z_0 is the only eigenfunction corresponding to propagating waves for a single-layer fluid. We therefore refer to Z_1 and Z_2 as the free-surface mode and the interfacial mode, respectively.

We remark that the asymptotic behaviour given for k_1 and k_2 is consistent with that obtained in the shallow-water case ($Kh \ll 1$) by Kelly (1969) and referred to in § 1.

3. An approximation

We use the eigenfunctions corresponding to propagating modes for a horizontal bed to approximate the solution ϕ for a varying bed by setting

$$\phi(x, y, z) \approx \psi(x, y, z) = \psi_1(x, y)Z_1(h(x, y), z) + \psi_2(x, y)Z_2(h(x, y), z). \tag{3.1}$$

The functions ψ_1 and ψ_2, which are to be determined, are required to be continuous in order that the approximations to the free-surface and interface elevations, obtained on replacing ϕ by ψ in (2.2), are continuous. Thus we represent $\psi \approx \phi$ by the propagating separation solutions at each x, y; the wavenumber $k_i = k_i(x, y)$ arising in the definition (2.6) of $Z_i(h(x, y), z)$ is the appropriate local solution of (2.8) where the depth is $h(x, y)$. The approximation therefore requires that the function $h(x, y)$ be slowly varying, in the sense that $\nabla_h h / k_1 h = O(\epsilon)$, where $\epsilon \ll 1$.

Because the dependence of ψ on the vertical coordinate is prescribed in (3.1) at each (x, y), when the variational principle $\delta L = 0$ is applied, z is removed by integration and equations for ψ_1 and ψ_2 are determined. To implement this process, we can assume that $\delta\psi_i = 0$ on $\mathscr{C}$ as we are not concerned for the moment with conditions on lateral boundaries but only with integration through the depth. Appropriate radiation conditions for the equations that result from this process will be identified in due course, independently of the vertical averaging. We also note from (2.5) that ψ satisfies the free-surface boundary condition, the interfacial conditions and $\psi_z = 0$ on $z = -h$. Using this information it follows from (2.3) that

$$\delta L = -2\mathrm{Re}\int\int_D \{(\nabla^2\psi, \delta\psi) + \rho^-[\delta\overline{\psi}\nabla_h h \cdot \nabla_h \psi]_{z=-h}\}\,\mathrm{d}x\,\mathrm{d}y.$$

https://doi.org/10.1017/S0022112004002356 Published online by Cambridge University Press

We require that L be stationary with respect to arbitrary variations in ψ_1 and ψ_2 (that vanish on $\mathscr{C} \times [-h, 0]$) and it can be shown when (3.1) is substituted that $\delta L = 0$ leads to

$$\sum_{i=1}^{2} \{(\nabla^2(Z_i\psi_i), Z_j) + \rho^-[Z_j \nabla_h h \cdot \nabla(Z_i\psi_i)]_{z=-h}\} = 0, \tag{3.2}$$

for $j = 1, 2$. After some manipulation this pair of differential equations for ψ_1 and ψ_2 can be written in the form

$$\sum_{i=1}^{2} \big\{\nabla_h \cdot (Z_i, Z_j)\nabla_h\psi_i + \{(\dot{Z}_i, Z_j) - (\dot{Z}_j, Z_i)\}\nabla_h h \cdot \nabla_h\psi_i + \big((Z_i'', Z_j) + (\dot{Z}_i, Z_j)\nabla_h^2 h + \{(\dot{Z}_i, Z_j)^{\cdot} - (\dot{Z}_i, \dot{Z}_j)\}(\nabla_h h)^2\big)\psi_i\big\} = 0, \tag{3.3}$$

for $j = 1, 2$, in which the prime denotes differentiation with respect to z, as in (2.5), and we have introduced the overdot to denote differentiation with respect to h.

We have not made use of the orthogonality of Z_1 and Z_2 or the property $Z_i'' = k_i^2 Z_i$ for $i = 1, 2$ in (3.3), for a reason that will become clear shortly. When these simplifications are incorporated, the pair of coupled equations is the counterpart for a two-layer fluid of the modified mild-slope equation derived by Chamberlain & Porter (1995). Indeed it can be shown that the system (3.3) reduces to the modified mild-slope equation in the single-layer limits, because (2.8) has been arranged to ensure that $Z_2 \to 0$ in these limits as described earlier.

As in the case of the modified mild-slope equation, (3.3) only applies where $\nabla_h^2 h$ exists. The variational principle remains valid where $\nabla_h h$ is discontinuous but the pointwise natural condition (3.2) cannot be deduced from $\delta L = 0$. Instead of modifying the functional L to deal with this situation we can simply integrate (3.3) across a line of discontinuity of $\nabla_h h$. Thus we find that the differential equations have to be replaced by the pair of coupled jump conditions

$$\sum_{i=1}^{2} (Z_i, Z_j)[\boldsymbol{n} \cdot \nabla_h\psi_i] + [\boldsymbol{n} \cdot \nabla_h h] \sum_{i=1}^{2} (\dot{Z}_i, Z_j)\psi_i = 0 \quad (j = 1, 2), \tag{3.4}$$

on such a line, [ ] denoting the jump in the included quantity and $\boldsymbol{n}$ a unit normal to the line. It follows that the approximations to the surface and interface elevations resulting from (3.1) have slope discontinuities where the bed does.

The approximation (3.1) can therefore be determined by solving (3.3) for ψ_1 and ψ_2 or, if necessary, obtaining piecewise solutions linked by (3.4). We shall describe how this process can be carried out for two-dimensional scattering in § 4.

Porter (2003) has recently noted that removing the term $\nabla_h^2 h$ from the modified mild-slope equation by a scaling has an overall simplifying effect as well as obviating the need to obtain solutions of the equation on subdomains and connected by jump conditions.

We therefore carry out the corresponding step in the present case and this can be achieved efficiently in the following way. Suppose that we replace the functions ψ_1 and ψ_2 by χ_1 and χ_2 through the transformation

$$(\psi_1\ \psi_2)^T = S(h)(\chi_1\ \chi_2)^T, \tag{3.5}$$

where $S(h)$ is a 2×2 matrix. Then the approximation (3.1) can be written as

$$\phi \approx \psi = (\psi_1\ \psi_2)(Z_1\ Z_2)^T = (\chi_1\ \chi_2)(Q_1\ Q_2)^T, \quad (Q_1\ Q_2) = (Z_1\ Z_2)S(h). \tag{3.6}$$

https://doi.org/10.1017/S0022112004002356 Published online by Cambridge University Press

Thus (3.1) is transformed to $\phi \approx \psi = \chi_1 Q_1 + \chi_2 Q_2$, where Q_1 and Q_2 are linear combinations of Z_1 and Z_2 still to be chosen, and the variational principle can be applied to this new version of ψ rather than to that given by (3.1). However, a new calculation is not required as Q_1 and Q_2 inherit all of the properties of Z_1 and Z_2 that were used to derive (3.3). Thus, $\delta L = 0$ applied to $\psi = \chi_1 Q_1 + \chi_2 Q_2$, where we assume that variations in χ_1 and χ_2 vanish on $\mathscr{C}$, gives a revised version of (3.3), in which ψ_i and Z_i are simply replaced by χ_i and Q_i, respectively, for $i = 1, 2$.

We now choose the transformation matrix $S(h)$ so that $(Q_i, \dot{Q}_j) = 0$ for $i, j = 1, 2$ which removes the term $\nabla_h^2 h$ from the revised form of (3.3) and reduces it to

$$\sum_{i=1}^{2} \{\nabla_h \cdot (Q_i, Q_j)\nabla_h \chi_i + ((Q_i'', Q_j) - (\dot{Q}_i, \dot{Q}_j)(\nabla_h h)^2)\chi_i\} = 0, \tag{3.7}$$

for $j = 1, 2$. The solutions χ_1 and χ_2 of this pair of equations are required to be continuous and have continuous first derivatives everywhere. The discontinuities in $\nabla\psi_i$ remain, of course, and arise through

$$(\nabla_h \psi_1 \ \nabla_h \psi_2)^T = \dot{S}(h)(\chi_1 \ \chi_2)^T \nabla_h h + S(h)(\nabla_h \chi_1 \ \nabla_h \chi_2)^T,$$

which follows from (3.5).

To make use of (3.7), the inner products involving Q_1 and Q_2 must be determined and these involve the matrix $S(h)$. Using (3.6), we find that the conditions $(Q_i, \dot{Q}_j) = 0$ for $i, j = 1, 2$ that determine $S(h)$ imply the matrix differential equation

$$U(h)\dot{S} + V(h)S = 0, \tag{3.8}$$

where $U = \mathrm{diag}(u_1, u_2)$ and V is the 2×2 matrix with i, j element v_{ij}, with

$$u_i(h) = ||Z_i||^2, \quad v_{ij}(h) = (Z_i, \dot{Z}_j).$$

It follows that $S(h) = (\boldsymbol{S}_1 \ \boldsymbol{S}_2)$, where the vectors $\boldsymbol{S}_1$ and $\boldsymbol{S}_2$ are linearly independent solutions of $U(h)\dot{\boldsymbol{S}} + V(h)\boldsymbol{S} = \boldsymbol{0}$. In scalar form, the components of $\boldsymbol{S} = (S_1 \ S_2)^T$ satisfy

$$\left.\begin{aligned} u_1 \dot{S}_1 + v_{11} S_1 + v_{12} S_2 = 0, \\ u_2 \dot{S}_2 + v_{21} S_1 + v_{22} S_2 = 0. \end{aligned}\right\} \tag{3.9}$$

An efficient way of evaluating inner products involving the functions Z_i and their h-derivatives is given in the appendix. In particular, it is shown there that

$$\dot{u}_i = 2v_{ii} - 2u_i \dot{k}_i / k_i, \quad k_1^2 v_{12} + k_2^2 v_{21} = 0,$$

which allow (3.9) to be reduced easily to

$$\dot{T}_1 + r(h) T_2 = 0, \quad \dot{T}_2 - r(h) T_1 = 0, \quad r(h) = k_1 v_{12} / k_2 (u_1 u_2)^{1/2},$$

where $T_i = k_i u_i^{1/2} S_i$. A straightforward integration now gives the solutions for T_1 and T_2 in the forms

$$T_1 = c_1 \cos\theta - c_2 \sin\theta, \quad T_2 = c_2 \cos\theta + c_1 \sin\theta, \quad \dot{\theta}(h) = r(h).$$

We take

$$S(h) = \begin{pmatrix} k_1 u_1^{1/2} & 0 \\ 0 & k_2 u_2^{1/2} \end{pmatrix}^{-1} \begin{pmatrix} \cos\theta & -\sin\theta \\ \sin\theta & \cos\theta \end{pmatrix} \tag{3.10}$$

which satisfies

$$S^T(h) \begin{pmatrix} k_1^2 u_1 & 0 \\ 0 & k_2^2 u_2 \end{pmatrix} S(h) = I. \tag{3.11}$$

https://doi.org/10.1017/S0022112004002356 Published online by Cambridge University Press

The coefficients in (3.7) can now be evaluated as follows. We use A and B to denote the 2×2 matrices with i, j components a_{ij} and b_{ij}, where

$$a_{ij} = (Q_i, Q_j), \quad b_{ij} = (\dot{Q}_i, \dot{Q}_j) \quad (i, j = 1, 2). \tag{3.12}$$

Since $\boldsymbol{Q} = S^T \boldsymbol{Z}$ from (3.6), the matrix with i, j component (Q_i, Q_j) is obtained by integrating $\boldsymbol{Q}\boldsymbol{Q}^T = S^T \boldsymbol{Z}\boldsymbol{Z}^T S$ through the depth and this at once gives

$$A = S^T U S. \tag{3.13}$$

Similarly, $\boldsymbol{Q}''\boldsymbol{Q}^T = S^T \boldsymbol{Z}''\boldsymbol{Z}^T S$ and using $Z_i'' = k_i^2 Z_i$ for $i = 1, 2$ and integrating shows that $(Q_i'', Q_j) = \delta_{ij}$, because of (3.11). Finally, we have $\dot{\boldsymbol{Q}} = S^T(\dot{\boldsymbol{Z}} - V^T U^{-1} \boldsymbol{Z})$ on using (3.8) to eliminate $\dot{S}$. Therefore

$$\dot{\boldsymbol{Q}}\dot{\boldsymbol{Q}}^T = S^T\{\dot{\boldsymbol{Z}}\dot{\boldsymbol{Z}}^T - \dot{\boldsymbol{Z}}\boldsymbol{Z}^T U^{-1} V - V^T U^{-1} \boldsymbol{Z}\dot{\boldsymbol{Z}}^T + V^T U^{-1} \boldsymbol{Z}\boldsymbol{Z}^T U^{-1} V\} S.$$

Integrating this equation over the depth we obtain

$$B = S^T(W - V^T U^{-1} V) S. \tag{3.14}$$

Here V and W are the matrices with i, j components v_{ij} and $w_{ij} = (\dot{Z}_i, \dot{Z}_j)$.

The system for χ_1 and χ_2 may therefore be written as

$$\sum_{i=1}^{2} \{\nabla_h \cdot a_{ij} \nabla_h \chi_i + (\delta_{ij} - b_{ij}(\nabla_h h)^2)\chi_i\} = 0, \tag{3.15}$$

for $j = 1, 2$, where a_{ij} and b_{ij} are expressed in terms of inner products of Z_1 and Z_2 and their derivatives with respect to h through the formulae for A and B given in (3.13) and (3.14).

It is not difficult to show that the components of A and B are invariant under arbitrary scalings of the eigenfunctions Z_i. More precisely, a_{ij} and b_{ij} are unaltered if Z_i is replaced by $c_i(h)Z_i$, where c_i is non-vanishing and differentiable for $i = 1, 2$. This is significant because it simplifies the calculation of the inner products (3.12). In the Appendix we give two ways in which a_{ij} and b_{ij} may be found. Firstly, we do not exploit the scale invariance of Z_i, and this approach gives expressions for the inner products appearing in (3.3). Secondly, we note that a_{ij} and b_{ij} are insensitive to changes in the coefficients α and β in (2.6), as long as α/β is unchanged. In particular, scaling (2.6) so as to replace β by unity gives rise to a considerable saving when implementing (3.7) or (3.17). An alternative approach is to approximate the inner products by a numerical quadrature. We have compared the exact values of a_{ij} and b_{ij} with those obtained by quadrature and found that they agree to within the accuracy of the numerical method.

The system (3.15) is the analogue of the revised form of the modified mild-slope equation derived by Porter (2003). It is a simplification of (3.3), requiring only the evaluation of

$$\theta(h) = \int_{\widetilde{h}}^{h} r(s)\,\mathrm{d}s \tag{3.16}$$

in addition to the quantities occurring in the original system, where $\widetilde{h}$ is an arbitrary reference depth.

https://doi.org/10.1017/S0022112004002356 Published online by Cambridge University Press

The main virtue of (3.15), however, is that if terms of $O(\epsilon^2)$ are discarded (ϵ being the mild-slope parameter introduced earlier) it reduces to

$$\left.\begin{aligned}\nabla_h\cdot a_{11}\nabla_h\chi_1+\nabla_h\cdot a_{12}\nabla_h\chi_2+\chi_1=0,\\ \nabla_h\cdot a_{12}\nabla_h\chi_1+\nabla_h\cdot a_{22}\nabla_h\chi_2+\chi_2=0,\end{aligned}\right\} \tag{3.17}$$

which avoids the need to evaluate v_{ij} and w_{ij}, except for v_{12} which arises in $\theta(h)$. Indeed, the coefficients in (3.17) are simply

$$a_{11}=k_1^{-2}\cos^2\theta+k_2^{-2}\sin^2\theta,\quad a_{22}=k_1^{-2}\sin^2\theta+k_2^{-2}\cos^2\theta,$$
$$a_{12}=a_{21}=\left(k_2^{-2}-k_1^{-2}\right)\cos\theta\sin\theta,$$

which show how $\theta(h)$ controls the coupling between the two wave modes. In the single-layer limits, (3.17) reduces to the corresponding equation for a single layer derived by Porter (2003), namely,

$$\nabla_h\cdot k^{-2}\nabla_h\chi_1+\chi_1=0.$$

In particular, the model therefore applies if the bed passes through the interface.

On the basis of an analysis of the single-layer case by Porter (2003), we can expect that the dominant contribution to the solution of (3.3) will not generally be given by discarding its higher-order terms. The system (3.17) will give the leading-order terms in ϵ of the solution of (3.15), however, and can be expected to produce good approximations. A numerical comparison of the solutions of (3.3) and (3.17) that substantiates this remark in a particular problem area will be given in the next section.

4. Two-dimensional scattering

To illustrate and compare the approximations that we have derived, we now restrict our attention to the case where $h=h(x)$ varies only for $x\in(0,\ell)$ and the motion is independent of y. We suppose that h' is continuous except, possibly, at $x=0$ or $x=\ell$. In this case we may write

$$\psi(x,z)=\psi_1(x)Z_1(h(x),z)+\psi_2(x)Z_2(h(x),z)$$

where

$$\psi_j(x)=\begin{cases}A_j^-\mathrm{e}^{\mathrm{i}k_j(h(0))x}+B_j^-\mathrm{e}^{-\mathrm{i}k_j(h(0))x}, & x<0,\\ B_j^+\mathrm{e}^{\mathrm{i}k_j(h(\ell))(x-\ell)}+A_j^+\mathrm{e}^{-\mathrm{i}k_j(h(\ell))(x-\ell)}, & x>\ell\end{cases} \tag{4.1}$$

($j=1,2$). There are, in general, four different wavenumbers here: k_1 and k_2 at each of $h=h(0)$ and $h=h(\ell)$.

In (4.1) coefficients $A_j^{\pm}$ are related to prescribed incident waves, and $B_j^{\pm}$ to scattered waves. We denote this situation by the row vector

$$\psi\sim\{\boldsymbol{a}^T\ ;\ \boldsymbol{b}^T\}\equiv\{A_1^-,A_2^-,A_1^+,A_2^+;\ B_1^-,B_2^-,B_1^+,B_2^+\}. \tag{4.2}$$

Four scattering problems, each corresponding to retaining just one of the four incident waves, can be defined using this shorthand notation by

$$\left.\begin{aligned}\psi^{(1)}&\sim\{1,0,0,0;R_{11}^-,R_{21}^-,T_{11}^-,T_{21}^-\},\\ \psi^{(2)}&\sim\{0,1,0,0;R_{12}^-,R_{22}^-,T_{12}^-,T_{22}^-\},\\ \psi^{(3)}&\sim\{0,0,1,0;T_{11}^+,T_{21}^+,R_{11}^+,R_{21}^+\},\\ \psi^{(4)}&\sim\{0,0,0,1;T_{12}^+,T_{22}^+,R_{12}^+,R_{22}^+\},\end{aligned}\right\} \tag{4.3}$$

https://doi.org/10.1017/S0022112004002356 Published online by Cambridge University Press

and we will assume later that this superscript notation for ψ is inherited by ψ_1 and ψ_2. (The notation in (4.3) is similar to that used by Linton & McIver (1995), but we have reordered the coefficients in anticipation of the notation introduced below.) In these definitions of the sixteen scattering coefficients, $R_{ij}^{\pm}$ refers to the reflected wave of wavenumber k_i due to an incident wave from $\pm\infty$ of wavenumber k_j. Coefficients involving T correspond to transmitted waves, labelled in the same way.

Guided by the structure of (4.3) we define $\Psi = (\psi^{(1)}, \psi^{(2)}\psi^{(3)}, \psi^{(4)})^T$ and write

$$\Psi \sim \{I_4 \ ; \ \mathscr{S}^T\},$$

where I_n denotes the $n \times n$ identity matrix and where $\mathscr{S}$ is the scattering matrix such that $\boldsymbol{b} = \mathscr{S}\boldsymbol{a}$. This definition of Ψ allows us to recover the general situation of (4.2) as a linear combination of the four basic scattering problems, for

$$\psi = \boldsymbol{a}^T\Psi \sim \boldsymbol{a}^T\{I_4 \ ; \ \mathscr{S}^T\} = \{\boldsymbol{a}^T \ ; \ (\mathscr{S}\boldsymbol{a})^T\} = \{\boldsymbol{a}^T \ ; \ \boldsymbol{b}^T\}.$$

Notice that we can construct $\overline{\Psi}$ in two different ways. Firstly, complex conjugation interchanges the roles of incident and scattered waves and we see that

$$\overline{\Psi} \sim \{\overline{\mathscr{S}^T} \ ; \ I_4\}.$$

We can replicate the set of incident waves appearing in $\overline{\Psi}$ by considering

$$\overline{\mathscr{S}^T}\Psi \sim \{\overline{\mathscr{S}^T} \ ; \ \overline{\mathscr{S}^T}\mathscr{S}^T\},$$

which must therefore have a left-hand side equal to $\overline{\Psi}$. It follows that

$$\mathscr{S}\overline{\mathscr{S}} = I_4, \tag{4.4}$$

which is an identity we will discuss later in this section.

4.1. *Numerical solutions*

We will consider results due to the original model (3.3), its scaled equivalent (3.15) and the simplified short version (3.17). We will begin with a general discussion and then give details relating to the specific cases at the end of this subsection.

The second-order system of equations can be written as a first-order system by defining $\boldsymbol{y} = [\boldsymbol{\psi}, U\boldsymbol{\psi}']^T$ in the case of equation (3.3) or $\boldsymbol{y} = [\boldsymbol{\chi}, A\boldsymbol{\chi}']^T$ for (3.15) or (3.17). In either case we have a first-order system which may be written

$$\boldsymbol{y}' = \mathscr{M}\boldsymbol{y}. \tag{4.5}$$

Eliminating the scattered wave terms from evaluations of (4.1) and their derivatives gives boundary conditions which must be satisfied by $\boldsymbol{y}$. These conditions may be written

$$P\boldsymbol{y}(0) = 2G_0\begin{pmatrix} A_1^- \\ A_2^- \end{pmatrix}, \qquad Q\boldsymbol{y}(\ell) = -2G_1\begin{pmatrix} A_1^+ \\ A_2^+ \end{pmatrix}. \tag{4.6}$$

Explicit expressions for the 2×4 matrices P and Q and the square matrices G_0 and G_1 are given later. We numerically approximate the solution of (4.5) and (4.6) by approximating linearly independent solutions of four real-valued initial value problems $\boldsymbol{y}_j' = \mathscr{M}\boldsymbol{y}_j$ (with $\boldsymbol{y}_j(0)$ assigned), $j = 1, 2, 3, 4$ and then constructing the required solution as a linear combination of this basis of solutions. This leads to

$$\boldsymbol{y}(x) = 2Y(x)N\boldsymbol{a} \quad \text{where} \quad N = \begin{pmatrix} PY(0) \\ QY(\ell) \end{pmatrix}^{-1}\begin{pmatrix} G_0 & 0 \\ 0 & -G_1 \end{pmatrix} \tag{4.7}$$

in which $Y = [\boldsymbol{y}_1, \boldsymbol{y}_2, \boldsymbol{y}_3, \boldsymbol{y}_4]$. In numerical results shown later we make the choice $Y(0) = I_4$, the 4×4 identity matrix, but we do not exploit that simplification here.

https://doi.org/10.1017/S0022112004002356 Published online by Cambridge University Press

Eliminating the incident wave terms from evaluations of (4.1) and their derivatives gives expressions for the scattered coefficients which may be written as

$$-2G_0\begin{pmatrix}B_1^-\\B_2^-\end{pmatrix}=\overline{P}\,\boldsymbol{y}(0),\qquad 2G_1\begin{pmatrix}B_1^+\\B_2^+\end{pmatrix}=\overline{Q}\,\boldsymbol{y}(\ell). \tag{4.8}$$

We can combine (4.7) and (4.8) to find the scattered coefficients $B_{1,2}^{\pm}$ in terms of the incident coefficients $A_{1,2}^{\pm}$ by

$$\boldsymbol{b}=\overline{N^{-1}N}\,\boldsymbol{a}$$

and therefore $\overline{N^{-1}N}$ is equal to the scattering matrix

$$\mathscr{S}=\begin{pmatrix}R_{11}^- & R_{12}^- & T_{11}^+ & T_{12}^+\\ R_{21}^- & R_{22}^- & T_{21}^+ & T_{22}^+\\ T_{11}^- & T_{12}^- & R_{11}^+ & R_{12}^+\\ T_{21}^- & T_{22}^- & R_{21}^+ & R_{22}^+\end{pmatrix}=\begin{pmatrix}R_- & T_+\\ T_- & R_+\end{pmatrix}\quad\text{(say)}. \tag{4.9}$$

Each column of $\mathscr{S}$ is related to one of the four scattering problems. Each row of $\mathscr{S}$ is related to one of the four scattered wavenumbers; for example the second row is related to left-travelling waves of wavenumber $k_2(h(0))$. The 2×2 matrices $R_{\pm}$ and $T_{\pm}$ each gather together scattering coefficients of a particular type (that is, reflection or transmission) due to wave incidence from a particular direction (that is, from $\pm\infty$).

4.1.1. *Equation* (3.3)

We allow h' to be discontinuous only at $x=0$ and $x=\ell$. Therefore when using (3.3) we must take note of the jump condition satisfied by $\boldsymbol{\psi}'$, which is

$$U[\boldsymbol{\psi}']+V[h']\boldsymbol{\psi}=\boldsymbol{0}, \tag{4.10}$$

and this leads to appearances of h' in

$$P=[G_0+V_0h'(0+),\,I_2],\quad Q=[-G_1+V_1h'(\ell-),\,I_2].$$

Here $G=\mathrm{i}\,\mathrm{diag}(k_1u_1,k_2u_2)$; a subscript zero (on G or V) implies evaluation at $h=h_0$ and a subscript 1 implies evaluation at $h=h(\ell)$.

4.1.2. *Equations* (3.15) *and* (3.17)

In these cases there are no jump conditions to consider, for $\boldsymbol{\chi}'$ is continuous even when h' is not. We find that

$$P=[G_0S_0,\,I_2],\quad Q=[-G_1S_1,\,I_2]$$

in which $G=\mathrm{i}\,S^T\mathrm{diag}(k_1u_1,k_2u_2)$ and where subscripts on G and now S have the same meaning as they did in §4.1.1. Observe that the matrix S now makes an appearance as a consequence of equation (3.5).

4.1.3. *Numerical procedure*

We now summarise the procedure implemented to produce the numerical results presented later. As mentioned above, we require numerical solutions to the four initial value problems

$$\boldsymbol{y}_j'=\mathscr{M}\,\boldsymbol{y}_j\quad(0<x<\ell),\qquad \boldsymbol{y}_j(0)\ \text{ given}$$

($j=1,2,3,4$) and this is achieved by standard means (see, for example, Lambert (1992)).

https://doi.org/10.1017/S0022112004002356 Published online by Cambridge University Press

Given (approximations to) $\boldsymbol{y}_j$ it is a simple matter to approximate N as defined in (4.7) and hence obtain approximations to the 16 scattering coefficients in $\mathscr{S} = \overline{N^{-1}}N$.

It is also possible to use the four numerical solutions to approximate the free surface and interface profiles in $0 < x < \ell$. This is achieved on using (4.7) to recall that $\boldsymbol{y} = 2YN\boldsymbol{a}$ is the solution to (4.5). In the case of (3.3) the first two entries of $\boldsymbol{y}$ are ψ_1 and ψ_2 leading to a direct calculation, *via* (3.1) of $\psi \approx \phi$. When using (3.15) or (3.17) the first two entries of $\boldsymbol{y}$ are χ_1 and χ_2. It is for this reason that there is some additional work to do if we require ψ. Equations (3.5), (3.10) and (3.16) show how this may be achieved and the only significant extra work is in approximating θ in order to construct $S(h)$. In this paper θ was approximated using a simple Gauss-Legendre quadrature. The reference level $\widetilde{h}$ was chosen to be the average of the maximum and minimum values of $h(x)$, so as to minimize the largest integration interval.

4.2. *Symmetry relations*

The reflection and transmission coefficients defined in (4.3) are connected by a set of so-called symmetry relations. Linton & McIver (1995) derived such a set of relations for the case in which the lower layer is of infinite extent. Their approach using Green's theorem can be applied in the present case to the original problem (2.1) and the relations thus derived coincide with (4.16) and (4.17) found below. The relations derived in this paper generalize those of Linton & McIver to the case where there are different finite depths at $x = \pm\infty$.

In order to derive symmetry relations for the scattering problems described above we suppose that $\boldsymbol{\psi}_a$ and $\boldsymbol{\psi}_b$ both satisfy (3.3), which may be written

$$(U\boldsymbol{\psi}')' + (V - V^T)h'\boldsymbol{\psi}' + X\boldsymbol{\psi} = \boldsymbol{0}, \tag{4.11}$$

where U and V are as previously given and where X may be inferred from (3.3). We could derive symmetry relations from (3.15) or (3.17), and the relations thus obtained agree with those that follow here. Also, there is some simplification when dealing with (3.15) or (3.17) since we do not need to implement a jump condition. However, in anticipation of the elements of U appearing in the symmetry relations, we will restrict our discussion to (3.3).

Consider

$$\mathscr{I} = \int_0^\ell \left(\boldsymbol{\psi}_a^T(U\boldsymbol{\psi}_b')' - \boldsymbol{\psi}_b^T(U\boldsymbol{\psi}_a')'\right) \mathrm{d}x. \tag{4.12}$$

It is a trivial matter to show that

$$\mathscr{I} = \left[\boldsymbol{\psi}_a^T U\boldsymbol{\psi}_b' - \boldsymbol{\psi}_b^T U\boldsymbol{\psi}_a'\right]_{0+}^{\ell-}. \tag{4.13}$$

Starting with (4.12) and using both (4.11) and the fact that $X - X^T = ((V - V^T)h')'$ we find that

$$\mathscr{I} = \left[\boldsymbol{\psi}_b^T(V - V^T)h'\boldsymbol{\psi}_a\right]_{0+}^{\ell-} = \left[\boldsymbol{\psi}_b^T Vh'\boldsymbol{\psi}_a - \boldsymbol{\psi}_a^T Vh'\boldsymbol{\psi}_b\right]_{0+}^{\ell-}$$

and this identity, taken with (4.10), implies that

$$\mathscr{I} = \left[\boldsymbol{\psi}_a^T U\boldsymbol{\psi}_b' - \boldsymbol{\psi}_b^T U\boldsymbol{\psi}_a'\right]_{0+}^{\ell-} - \left[\boldsymbol{\psi}_a^T U\boldsymbol{\psi}_b' - \boldsymbol{\psi}_b^T U\boldsymbol{\psi}_a'\right]_{0-}^{\ell+}. \tag{4.14}$$

Comparison of (4.13) and (4.14) gives the key result

$$\left[\boldsymbol{\psi}_a^T U\boldsymbol{\psi}_b' - \boldsymbol{\psi}_b^T U\boldsymbol{\psi}_a'\right]_{0-}^{\ell+} = 0. \tag{4.15}$$

Symmetry relations emerge on 'ringing the changes' among choices of $\boldsymbol{\psi}_a$ and $\boldsymbol{\psi}_b$ in (4.15), as we now go on to demonstrate.

https://doi.org/10.1017/S0022112004002356 Published online by Cambridge University Press

Choosing $\boldsymbol{\psi}_a = (\psi_1^{(m)}, \psi_2^{(m)})^T$ and $\boldsymbol{\psi}_b = \overline{(\psi_1^{(n)}, \psi_2^{(n)})^T}$ for $m, n = 1, 2, 3, 4$ in equation (4.15) yields ten equations (four real-valued and six complex-valued) which may be summarized as

$$\mathscr{S}^T J \overline{\mathscr{S}} = J, \tag{4.16}$$

where $J = \mathrm{diag}(q_1(0), q_2(0), q_1(\ell), q_2(\ell))$ in which $q_j(x) = k_j(h(x))u_j(h(x))$. The elements of J may be thought of as weighting terms related to waves of each of the four scattered wavenumbers. For example, the first element of J only ever multiplies elements in the top row of $\mathscr{S}$, these elements being those describing motion in $x < 0$ of wavenumber k_1.

The four equations implied by the diagonal elements of (4.16) lead to energy conservation in each of the four scattering problems and the complex conjugates of the six equations above the diagonal appear below the diagonal. It is informative to isolate the identities along the diagonal of (4.16); these energy conservation equations may be written

$$\begin{pmatrix} |R_{11}^-|^2 - 1 & |R_{21}^-|^2 & |T_{11}^-|^2 & |T_{21}^-|^2 \\ |R_{12}^-|^2 & |R_{22}^-|^2 - 1 & |T_{12}^-|^2 & |T_{22}^-|^2 \\ |T_{11}^+|^2 & |T_{21}^+|^2 & |R_{11}^+|^2 - 1 & |R_{21}^+|^2 \\ |T_{12}^+|^2 & |T_{22}^+|^2 & |R_{12}^+|^2 & |R_{22}^+|^2 - 1 \end{pmatrix} \begin{pmatrix} q_1(0) \\ q_2(0) \\ q_1(\ell) \\ q_2(\ell) \end{pmatrix} = \mathbf{0}.$$

Another six relations can be obtained by choosing $\boldsymbol{\psi}_a = (\psi_1^{(m)}, \psi_2^{(m)})^T$ and $\boldsymbol{\psi}_b = (\psi_1^{(n)}, \psi_2^{(n)})^T$ for $m, n = 1, 2, 3, 4$, and these six, complex-valued, relations may be written as

$$\mathscr{S}^T J = J \mathscr{S}. \tag{4.17}$$

The information given in (4.17) may be written in another way:

$$\begin{pmatrix} T_{11}^+ & 0 & -T_{11}^- & 0 \\ 0 & T_{22}^+ & 0 & -T_{22}^- \\ R_{12}^- & -R_{21}^- & 0 & 0 \\ 0 & 0 & R_{12}^+ & -R_{21}^+ \\ T_{12}^+ & 0 & 0 & -T_{21}^- \\ 0 & T_{21}^+ & -T_{12}^- & 0 \end{pmatrix} \begin{pmatrix} q_1(0) \\ q_2(0) \\ q_1(\ell) \\ q_2(\ell) \end{pmatrix} = \mathbf{0}.$$

The relations given in (4.17) are perhaps the ones most deserving the name 'symmetry'; for example, one of them states that (up to multiplication by the weighting elements of J) the transmission to the left of wavenumber $k_1(h(0))$ due to an incident wave of wavenumber $k_2(h(\ell))$ is the same as the transmission to the right of wavenumber $k_2(h(\ell))$ due to an incident wave of wavenumber $k_1(h(0))$. Three of the other relations state similar symmetries in the remaining transmission coefficients and there are two corresponding results concerning four of the reflection coefficients. No information is given in (4.17) concerning $R_{jj}^{\pm}$, $(j = 1, 2)$, the coefficients describing reflection of the wavenumber of the incident wave, because, clearly, (4.15) delivers no non-trivial information when $\boldsymbol{\psi}_a = \boldsymbol{\psi}_b$.

Next we discuss two other ways by which symmetry relations may be derived.

Earlier in this section we saw a proof that $\mathscr{S}\overline{\mathscr{S}} = I_4$. This identity is a consequence of (4.16) and (4.17) of course, but the derivation given earlier shows that (4.4) depends only on the far-field behaviour.

https://doi.org/10.1017/S0022112004002356 Published online by Cambridge University Press

Another approach that can be used to derive a symmetry relation involves a Wronskian. The fact that $\mathrm{tr}(\mathscr{M})=0$ implies that the corresponding Wronskian is a constant. Denoting $\boldsymbol{\psi}^{(n)}$, $n=1, 2, 3, 4$ as solutions of (4.11) it follows that

$$\left|\begin{matrix}\boldsymbol{\psi}^{(1)} & \boldsymbol{\psi}^{(2)} & \boldsymbol{\psi}^{(3)} & \boldsymbol{\psi}^{(4)} \\ U\boldsymbol{\psi}^{(1)\prime} & U\boldsymbol{\psi}^{(2)\prime} & U\boldsymbol{\psi}^{(3)\prime} & U\boldsymbol{\psi}^{(4)\prime}\end{matrix}\right|_{x=0-} = \left|\begin{matrix}\boldsymbol{\psi}^{(1)} & \boldsymbol{\psi}^{(2)} & \boldsymbol{\psi}^{(3)} & \boldsymbol{\psi}^{(4)} \\ U\boldsymbol{\psi}^{(1)\prime} & U\boldsymbol{\psi}^{(2)\prime} & U\boldsymbol{\psi}^{(3)\prime} & U\boldsymbol{\psi}^{(4)\prime}\end{matrix}\right|_{x=\ell+}, \tag{4.18}$$

since $U'=0$ in the two semi-infinite regions $x<0$ and $x>\ell$. Use of (4.1) and (4.3), followed by some row operations, allows us to evaluate these determinants and hence obtain the symmetry relation

$$q_1(0)q_2(0)(T_{21}^{+}T_{12}^{+}-T_{11}^{+}T_{22}^{+})=q_1(\ell)q_2(\ell)(T_{21}^{-}T_{12}^{-}-T_{11}^{-}T_{22}^{-}). \tag{4.19}$$

This gives us no new information, for (4.19) is a direct consequence of (4.17).

Symmetry relations can be used as a check on the accuracy of numerical results. It has been found that the error in (the approximated versions of) (4.16), (4.17) and (4.19) is of the same order as that incurred in the differential equation solver. This is not surprising, for these relations come from (4.15) and (4.18) which were derived using (4.11). Interestingly, (4.4) is always satisfied to machine accuracy, even if the differential equation solver is a very poor one, since the only information used to derive it is the far-field behaviour, in which the only numerical error will be due to rounding. Clearly, any errors in the entries of $\mathscr{S}$ cancel out in $\mathscr{S}\overline{\mathscr{S}}$, as long as the correct far-field behaviour is retained. Indeed this is clear because our numerical formulation involved the identity $\mathscr{S}=\overline{N^{-1}}N$, from which $\mathscr{S}\overline{\mathscr{S}}=I_4$ is immediate.

4.3. *Some numerical results*

Here we present some numerical results for the two-dimensional scattering problem that has been the subject of this section. One purpose of the investigation is to compare (3.3), (3.15) and (3.17).

It is convenient to introduce the notion of scaled scattering coefficients. These scaled coefficients all have absolute value in the interval $[0, 1]$ and it is therefore easier to see how the energy in the incident wave is distributed among the transmitted and reflected waves than it is when dealing with the elements of $\mathscr{S}$. We define the scattering matrix of scaled scattering coefficients to be

$$\tilde{\mathscr{S}}=J^{1/2}\mathscr{S}J^{-1/2}. \tag{4.20}$$

Notation for the individual sixteen elements of $\tilde{\mathscr{S}}$ is adopted by recalling (4.9) so that, for example, we write $(\tilde{\mathscr{S}})_{1,3}=\tilde{T}_{11}^{+}$, and so on. We note that the four reflection coefficients describing reflection at the wavenumber of the incident wave are unchanged by this scaling, that is $\tilde{R}_{jj}^{\pm}=R_{jj}^{\pm}$ for $j=1, 2$.

Symmetry relations satisfied by the elements of $\tilde{\mathscr{S}}$ arise from the equations

$$\tilde{\mathscr{S}}=\tilde{\mathscr{S}}^{T}=\overline{\tilde{\mathscr{S}}^{-1}}, \tag{4.21}$$

which are a consequence of (4.16), (4.17) and (4.20). Equations (4.21) imply several explicit identities involving the scaled scattering coefficients, but it serves our purpose to list only a few of them here. The absolute square column sums of $\tilde{\mathscr{S}}$ are all equal to one, or to put it another way,

$$\sum_{i=1}^{2}(|\tilde{R}_{ij}^{\pm}|^2+|\tilde{T}_{ij}^{\pm}|^2)=1 \qquad (j=1, 2) \tag{4.22}$$

https://doi.org/10.1017/S0022112004002356 Published online by Cambridge University Press

and symmetry of $\tilde{\mathscr{S}}$ implies that

$$\tilde{R}_{\pm} = \tilde{R}_{\pm}^{T}, \qquad \tilde{T}_{\pm} = \tilde{T}_{\mp}^{T}, \tag{4.23}$$

which lead to a further six identities. Equation (4.22) is an explicit statement of energy conservation for each of the four scattering problems defined in (4.3). The identities (4.23) are a restatement of (4.17) and reduce the number of scattering coefficients that need to be presented later.

Interestingly, (4.21) also implies that the absolute square row sums of $\tilde{\mathscr{S}}$ are all equal to 1 (this can also be seen by using (4.23) to restate each equation (4.22) as one involving scattering coefficients related to the same wavenumber), that is,

$$\sum_{j=1}^{2}(|\tilde{R}_{ij}^{\pm}|^2 + |\tilde{T}_{ij}^{\mp}|^2) = 1 \qquad (i = 1, 2). \tag{4.24}$$

The identities in (4.24) state that the energy transmitted at each wavenumber and in each direction, taken over all four scattering problems defined in (4.3), is equal to the energy in the incident wave at that wavenumber.

4.3.1. *Example 1: a symmetric profile*

In this example we consider the depth profile

$$h(x) = h(0)\left(\tfrac{3}{5} + \tfrac{2}{5}\cos(2\pi x/\ell)\right)$$

which has the property that $h(x) = h(\ell - x)$. This additional symmetry in the problem means that half the elements of $\tilde{\mathscr{S}}$ are equal to the other half, specifically $\tilde{R}_{+} = \tilde{R}_{-}$ and $\tilde{T}_{+} = \tilde{T}_{-}$. Confirming that this is the case for numerical approximations to these quantities provides an additional, if rather trivial, check on accuracy.

For this example we take $Kh(0) = 0.8$ and $Kd = 0.1$. We now give some thought to what values to take for ρ. Lamb (1932, Art 231, p. 371) refers to an example (water over mercury) in which $\rho^{-1} = 13.6$. More recent publications (for example Linton & McIver 1995 or Cadby & Linton 2000) mention an application of fresh water above salt water in which case $\rho \approx 0.95$. Recent results concerning wave trapping in an infinitely deep two-layer fluid considered by Linton & Cadby (2003) deal with ρ throughout the interval $(0, 1)$. In this example we consider three values of ρ: 0.1, 0.5 and 0.9.

Figure 1 shows the scattering coefficients for $K\ell$ between 2 and 10. For reasons of symmetry we only show quantities $|\tilde{R}_{ij}^{-}|$ and $|\tilde{T}_{ij}^{-}|$ (for $i, j = 1, 2$) and a further saving is possible since, from (4.23), $\tilde{R}_{12}^{-} = \tilde{R}_{21}^{-}$ and, as a further consequence of the topographic symmetry, $\tilde{T}_{12}^{-} = \tilde{T}_{21}^{-}$. Figure 1 shows approximations to the scattering coefficients for both the full model shown in (3.3) or (3.15) and also for the simplified model (3.17). The fact that two values are visible in very few places, for example $|\tilde{R}_{11}^{-}|$ for small values of $K\ell$, is an indication that the simplified model compares very favourably with the full model. We have found that this agreement between the two models is typical of all numerical computations that have been carried out.

More generally, a numerical investigation of the coefficients b_{ij} arising in (3.15) gives evidence that that $|b_{11}| < 0.031$, $|b_{12}| < 0.045$ and $|b_{22}| < 0.14$ for all values of ρ and all values of h and d corresponding to a situation where the lower layer accounts for at least 10% of the quiescent fluid depth. Therefore (3.17) provides an excellent approximation to (3.15) except, possibly, when the lower fluid layer is relatively thin, this being a case where the numerical evidence is less reliable due to the singular nature of the wavenumbers.

https://doi.org/10.1017/S0022112004002356 Published online by Cambridge University Press

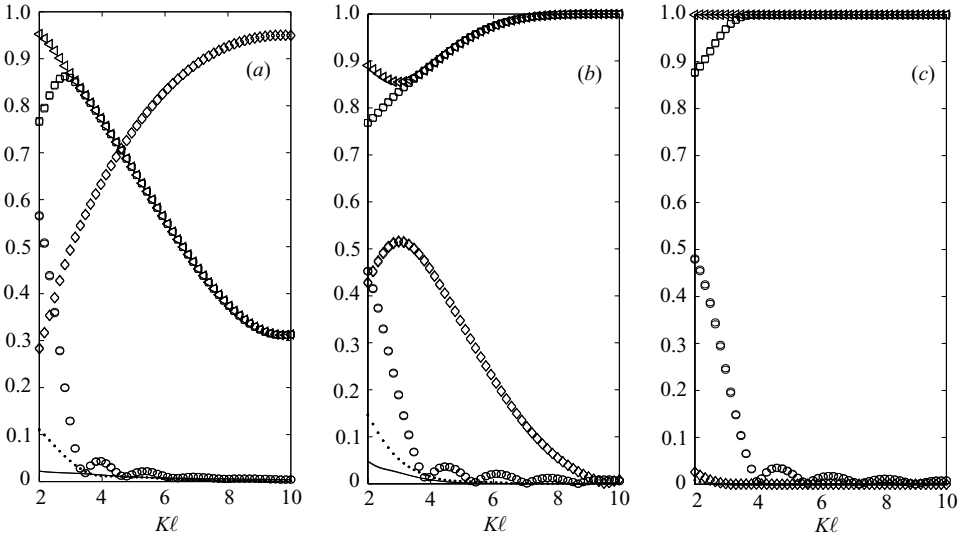


FIGURE 1. Absolute values of scattering coefficients for the symmetric topography. Quantities shown are $|\tilde{R}_{11}^{-}|$ (circles), $|\tilde{T}_{11}^{-}|$ (squares), $|\tilde{R}_{21}^{-}|$ (dots), $|\tilde{T}_{21}^{-}|$ (diamonds), $|\tilde{R}_{22}^{-}|$ (solid line) and $|\tilde{T}_{22}^{-}|$ (left-pointing triangles). Other scattering coefficients are equal to one of those shown, as a consequence of topographic symmetry and (4.23). (*a*) $\rho = 0.1$, (*b*) $\rho = 0.5$, (*c*) $\rho = 0.9$. In each case two approximations are shown, one corresponding to the full model (3.3) (or, equivalently, (3.15)) and one corresponding to the shorter, simplified model (3.17); however in most places the approximations are so close as to be indistinguishable.

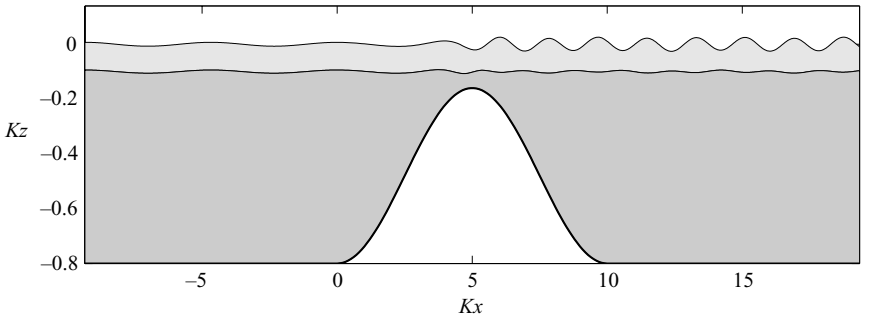


FIGURE 2. Snapshot of a wave profile above the symmetric topography for an incident wave from the left of wavenumber $k_1(h(0))$. Here $\rho = 0.1$ and $K\ell = 10$.

Towards the right of figure 1(*a*) we can see that $\tilde{T}_{21}^{-} = \tilde{T}_{12}^{-}$ is relatively large, and this means that energy is being transferred from one wavenumber to the other. Figure 2 shows the case where $\rho = 0.1$ and $K\ell = 10$ and shows a snapshot of the wave profile for the problem involving an incident wave from the left of wavenumber k_1. In this case $k_1(h(0))/K = 1.3454$ and $k_2(h(0))/K = 3.4562$, to four decimal places, which correspond to wavelengths of $4.6701/K$ and $1.8180/K$ respectively. In $x < 0$, the fact that $\tilde{R}_{11}^{-}$ and $\tilde{R}_{21}^{-}$ are small means that the wave motion is dominated by the incident wave, and this fact is evident since it is the longer wavelength that is apparent at the interface and the free surface. In $x > \ell$ the large value of $|\tilde{T}_{21}^{-}| \approx 0.95$ gives rise to wave motion that is dominated by the shorter wavelength.

https://doi.org/10.1017/S0022112004002356 Published online by Cambridge University Press

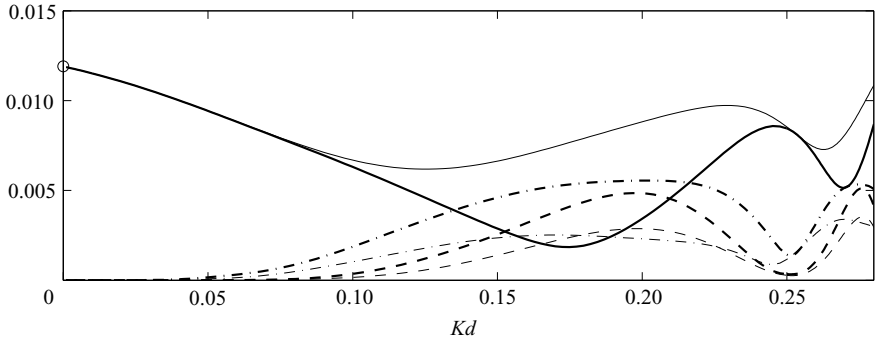


FIGURE 3. Absolute values, for the asymmetric topography, of the reflection coefficients for varying Kd. The solid lines show $|\tilde{R}^{\pm}_{11}|$, the dashed lines show $|\tilde{R}^{\pm}_{12}| = |\tilde{R}^{\pm}_{21}|$ and the dash-dot lines show $|\tilde{R}^{\pm}_{22}|$. In each case the heavier line represents the quantity with the + superscript. A circle on the vertical axis shows the corresponding value for the one-layer case.

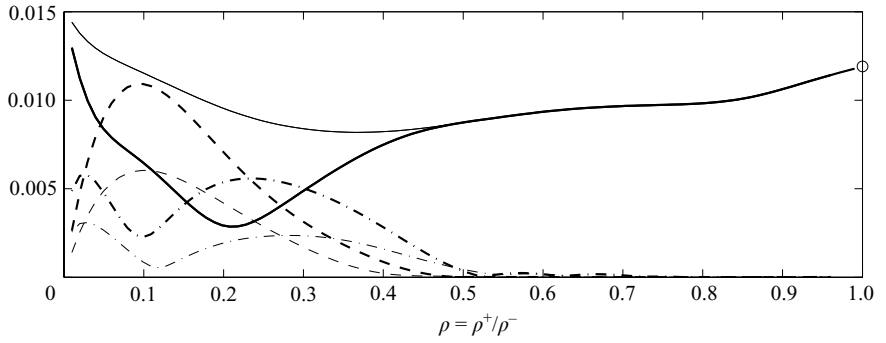


FIGURE 4. Absolute values, for the asymmetric topography, of the reflection coefficients for fixed $Kd = 0.2$ and varying ρ. The solid lines show $|\tilde{R}^{\pm}_{11}|$, the dashed lines show $|\tilde{R}^{\pm}_{12}| = |\tilde{R}^{\pm}_{21}|$ and the 'dash-dot' lines show $|\tilde{R}^{\pm}_{22}|$. In each case the heavier line represents the quantity with the + superscript. A circle on the line $\rho = 1$ shows the corresponding value for the one-layer case.

4.3.2. *Example 2: an asymmetric profile*

Here we choose $h(x) = h(0)(1 - (x/\ell)^2(15(x/\ell)^2 - 29(x/\ell) + \frac{27}{2}))$.

For the present example we make the following choices of parameters: $Kh(0) = 1$, $K\ell = 8$, $\rho = \rho^+/\rho^- = 0.25$, and we show how the six reflection coefficients vary with Kd. The depth has a global minimum of $0.2938/K$, to four decimal places, at $Kx = 0.45$ and Kd varies between 0.001 and 0.28 in figure 3.

It is of interest to note that we can use the modified mild-slope equation (mmse; see, for example, Chamberlain & Porter 1995) to approximate wave reflection in the one-layer problem for this asymmetric topography and we find that $|R_{\mathrm{mmse}}| = 0.0119$, to four decimal places. This value is shown as a circle on the vertical axis in figure 3 and we see that the one-layer limit of our two-layer results is as it should be with $|\tilde{R}^{\pm}_{11}| = |R^{\pm}_{11}|$ approaching $|R_{\mathrm{mmse}}|$. (The arguments of these two complex numbers also agree, but this is not shown in the figure.) Also, all of the reflection coefficients involving k_2 in any way (that is, those with a 2 in either subscript position) decay to zero in the limit $d \to 0$.

In figure 4, we fix $Kd = 0.2$ and vary ρ in the interval $(0, 1)$. In this case it is the limit $\rho \to 1$ which leads to the corresponding one-layer problem and the value

https://doi.org/10.1017/S0022112004002356 Published online by Cambridge University Press

$|R_{\mathrm{mmse}}| = 0.0119$ is indicated as a circle on the line $\rho = 1$. Once again we see that, in the limit $\rho \to 1$, $|R_{11}^{+}| \to |R_{\mathrm{mmse}}|$ and all of the reflection coefficients involving k_2 in either the incident or scattered wave tend to zero.

5. Conclusions

The work described in this paper is based on a variational principle that is equivalent to the solving the equations governing free-surface motions of a two-layer fluid over arbitrary bed undulations. When the principle is used in conjunction with the Rayleigh–Ritz method, solutions of the equations can be produced to any desired accuracy by choosing a large enough basis for the trial function.

Here we have used just a two-dimensional trial space based on the propagating wave modes for a flat bed, in order to derive a relatively simple approximation to scattering by slowly varying bedforms. As this choice of trial function leads to the elimination of the vertical coordinate, the approximation is determined by solving a pair of coupled partial differential equations in two independent variables. A further simplification arises following a transformation of the coupled system, which identifies terms that are negligible: they have coefficients of small magnitude and are second order in the bed slope, which is assumed to be small.

We therefore arrive at the reduced system (3.17), which contains the wavenumbers of the competing surface and interfacial modes, modulated by variations in the bed shape, and the angle θ, where

$$\theta(h) = \rho^{-} \int_{\tilde{h}}^{h} \frac{k_1 k_2 \beta_1 \beta_2}{\left(k_1^2 - k_2^2\right)\sqrt{u_1 u_2}}\, \mathrm{d}h,$$

which controls the relative weights of the wavenumbers. Numerical experiments have shown that (3.17) produces virtually the same results as the full system (3.3) or (3.15), except when the ratio of the depths of the fluid layers is very small. The full system reduces to the modified mild-slope equation of Chamberlain & Porter (1995) in the single-layer limits and, correspondingly, (3.17) reduces to the simpler mild-slope equation in the form recently derived by Porter (2003). Because the wavenumber of the internal wave tends to infinity in the single-layer limits, computations of cases in which the bed penetrates the interface have not so far been attempted. An approach which identifies the local analytic solution at the contact line in the neighbourhood of the interface and builds this into a numerical method will be likely to resolve such cases.

The accuracy of the approximation incurred by using a simple trial function can only be ascertained by returning to the variational principle and taking a larger basis by including the vertical eigenfunctions corresponding to evanescent modes. This process has been carried out for the single-layer mild-slope approximation by Porter & Staziker (1995) and Athanassoulis & Belibassakis (1999), who obtained superior convergence by a judicious choice of basis. These investigations and other evidence in the form of comparisons with experimental data and with full linear solutions obtained by other means, including that for periodic beds given recently by Porter & Porter (2003), indicates that the mild-slope approach provides a good approximation for free-surface motions, as long as the bedform gradient is not too large. On this basis, we believe that we have developed a reasonable first approximation in the present problem, at least for moderate bed slopes. However, it still remains to determine the limitations of our simple approximation in the present context, along the lines indicated above.

https://doi.org/10.1017/S0022112004002356 Published online by Cambridge University Press

The vertical averaging required in the implementation of the approximation results in a number of inner products for which we have devised a systematic evaluation procedure, obviating the need for lengthy expressions or expensive computations. This aspect of the work applies when a larger basis is used in the present problem as well as in other contexts.

We have illustrated the method by considering scattering in a two-dimensional context. Numerical evidence suggests that the most significant transfer of energy between the shorter and longer waves occurs when $\rho = \rho^+/\rho^-$ is nearer 0 than 1 or when the interface is not very near the free surface.

The equations that we have derived can equally be used to examine three-dimensional bedforms. One way of proceeding in this case is to convert (3.15) into a pair of coupled domain integral equations, which can be solved by collocation; Porter & Porter (2001) have successfully used this approach for the modified mild-slope equation.

Appendix

The purpose of this Appendix is to show how the inner products occurring in the differential equation systems may be determined by an efficient analytic approach. In § A 1 we set out the method for all of the inner products required in the main body of the text.

Section A 2 exploits a simplification that is possible if we are interested only in an implementation of either (3.15) or (3.17).

A 1. *Inner products*

We evaluate

$$u_i = ||Z_i||^2, \quad v_{ij} = (Z_i, \dot{Z}_j), \quad w_{ij} = (\dot{Z}_i, \dot{Z}_j) \quad (i, j = 1, 2).$$

Only u_i has to be determined by carrying out an integration, the result of this being

$$u_i = \frac{1}{4k_i}\{\rho^+\alpha_i^2\big[2Kk_i(1-\cosh 2k_i d) + 2k_i d\big(k_i^2 - K^2\big) + \big(k_i^2 + K^2\big)\sinh 2k_i d\big] + \rho^-\beta_i^2[2k_i(h-d) + \sinh 2k_i(h-d)]\},$$

where $\alpha_i = \alpha_i(h)$ and $\beta_i = \beta_i(h)$ are the coefficients defined in (2.7) evaluated for $k = k_i$.

We first observe that, as $Z_i(h, z)$ satisfies (2.5) with $\mu = k_i^2$, then

$$\dot{Z}_i'' = k_i^2\dot{Z}_i + 2k_i\dot{k}_i Z_i. \tag{A 1}$$

We also note from (2.6) that

$$[Z_i(h, z)]_{z=-h} = \beta_i, \quad [\dot{Z}_i'(h, z)]_{z=-h} = k_i^2\beta_i. \tag{A 2}$$

Now

$$\begin{aligned}(Z_i'', \dot{Z}_j) - (Z_i, \dot{Z}_j'') &= \rho^+[Z_i'\dot{Z}_j - \dot{Z}_j'Z_i]_{z=-d}^{z=0} + \rho^-[Z_i'\dot{Z}_j - \dot{Z}_j'Z_i]_{z=-h}^{z=-d}\\ &= \rho^- k_j^2\beta_i\beta_j,\end{aligned}$$

using (A 2), since $\dot{Z}_j$ satisfies the free-surface boundary condition and the interfacial conditions. Thus, from (2.5) and (A 1), we have

$$k_i^2(Z_i, \dot{Z}_j) - k_j^2(Z_i, \dot{Z}_j) - 2k_j\dot{k}_j(Z_i, Z_j) = \rho^- k_j^2\beta_i\beta_j. \tag{A 3}$$

https://doi.org/10.1017/S0022112004002356 Published online by Cambridge University Press

Two cases arise. For $i \neq j$, the orthogonality of Z_i and Z_j implies that

$$v_{ij} = \frac{\rho^- k_j^2 \beta_i \beta_j}{k_i^2 - k_j^2}, \tag{A 4}$$

and therefore

$$k_i^2 v_{ij} + k_j^2 v_{ji} = 0.$$

For $i = j$, (A 3) shows that

$$2\dot{k}_i u_i = -\rho^- k_i \beta_i^2, \qquad 2\ddot{k}_i u_i + 2\dot{k}_i \dot{u}_i = -\rho^- \big(\dot{k}_i \beta_i^2 + 2k_i \dot{\beta}_i \beta_i\big), \tag{A 5}$$

the second identity being the derivative of the first. Thus $\dot{k}_i$ is given in terms of known quantities, allowing $\dot{u}_i$, $\dot{\beta}_i$, $\ddot{k}_i$, $\ddot{u}_i$ and $\ddot{\beta}_i$ to be successively determined.

Now direct differentiation of the inner product with respect to h gives

$$(Z_i, Z_i)^{\cdot} = 2(Z_i, \dot{Z}_i) + \rho^- \beta_i^2,$$

and by virtue of (A 5) we therefore have

$$2v_{ii} = \dot{u}_i - \rho^- \beta_i^2, \qquad \dot{u}_i = 2v_{ii} - 2\dot{k}_i u_i / k_i, \tag{A 6}$$

the first equation giving v_{ii}; the second is used in the main body of the text.

This procedure may be extended. Since $[\dot{Z}_i(h, z)]_{z=-h} = \dot{\beta}_i$ follows from (2.6), we have

$$(\dot{Z}_i'', \dot{Z}_j) - (\dot{Z}_i, \dot{Z}_j'') = -\rho^- \big(k_i^2 \beta_i \dot{\beta}_j - k_j^2 \beta_j \dot{\beta}_i\big)$$

and using (A 1) this leads to

$$\big(k_i^2 - k_j^2\big) w_{ij} + 2k_i \dot{k}_i v_{ij} - 2k_j \dot{k}_j v_{ji} = -\rho^- \big(k_i^2 \beta_i \dot{\beta}_j - k_j^2 \beta_j \dot{\beta}_i\big).$$

Thus w_{ij} is given in terms of quantities determined above, for $i \neq j$.

To derive an expression for w_{ii}, we differentiate the first element of (A 6) to give

$$2w_{ii} + 2(Z_i, \ddot{Z}_i) = \ddot{u}_i - 4\rho^- \beta_i \dot{\beta}_i. \tag{A 7}$$

Evaluating $(\dot{Z}_i'', \ddot{Z}_i) - (\dot{Z}_i, \ddot{Z}_i'')$ by following the routine that led to (A 3), we readily find that

$$2k_i \dot{k}_i (Z_i, \ddot{Z}_i) - 4k_i \dot{k}_i w_{ii} - 2(k_i \dot{k}_i)^{\cdot} v_{ii} = -\rho^- \big\{k_i^2 \beta_i \big(\ddot{\beta}_i + k_i^2 \beta_i\big) - \dot{\beta}_i \big(2k_i^2 \dot{\beta}_i + 4k_i \dot{k}_i \beta_i\big)\big\},$$

and elimination of $(Z_i, \ddot{Z}_i)$ between this equation and (A 7) gives w_{ii}.

It is perhaps worth remarking that, although these various identities may appear to be involved, the direct evaluation and simplification of the integrals defining v_{ij} and w_{ij} is a formidable exercise, which the above approach explicitly avoids and replaces by a sequence of relationships. Reference to Silva *et al.* (2002) shows the level of complexity that can arise from calculations of this type if some indirect strategy is not devised.

A 2. *Scale invariance*

In § A 1 we saw how to evaluate the inner products for the original model (3.3), its scaled equivalent (3.15) and the simple model (3.17). There is a simpler way of finding the inner products required for the second and third of these, and the simplification is due to a scale invariance. The coefficients in (3.15) are insensitive to the way in which the functions Z_i are scaled. We therefore redefine those functions and take

$$\left.\begin{aligned} Z(h, z) &= \alpha\beta^{-1}\{k \cosh(kz) + K \sinh(kz)\} && (-d < z \leqslant 0), \\ &= \cosh k(z + h) && (-h \leqslant z \leqslant -d). \end{aligned}\right\}$$

https://doi.org/10.1017/S0022112004002356 Published online by Cambridge University Press

This has the advantage that, in a rederivation of the § A 1 calculations, there will be no appearance of $\dot{\beta}$ or $\ddot{\beta}$.

The inner product $u_i = ||Z_i||^2$ is not scale invariant and must be recomputed, the way in which it changes is trivial and we now find that

$$u_i = \frac{1}{4k_i}\{\rho^+\alpha_i^2\beta_i^{-2}[2Kk_i(1-\cosh 2k_i d) + 2k_i d(k_i^2 - K^2) + (k_i^2 + K^2)\sinh 2k_i d] + \rho^-[2k_i(h-d) + \sinh 2k_i(h-d)]\}.$$

The method of § A 1 can now be reapplied. The functions $Z_i(h, z)$ satisfy equations (A 1), (A 2), (A 3) and (A 4) where β_i and β_j are each replaced with the constant 1. We deduce that

$$v_{ij} = \frac{\rho^- k_j^2}{k_i^2 - k_j^2},$$

for $i \neq j$ and

$$2v_{ii} = \dot{u}_i - \rho^-,$$

which, of course, are not scale invariant.

This leaves us to find only the inner products w_{ij}, which are required for (3.15), but not for the simplified model (3.17). For $i \neq j$ this is achieved *via*

$$(k_i^2 - k_j^2)w_{ij} + 2k_i\dot{k}_i v_{ij} - 2k_j\dot{k}_j v_{ji} = 0,$$

and for $i = j$ we use

$$2w_{ii} + 2(Z_i, \ddot{Z}_i) = \ddot{u}_i.$$

It follows that

$$A = S^T U S, \qquad B = S^T(W - V^T U^{-1} V)S,$$

and we emphasise that, as a result of the scale invariance, the left hand sides of these expressions will be equal to those in (3.13) and (3.14). In general, none of the separate elements on the right hand sides will be equal to their § A 1 counterparts.

In the interests of being absolutely explicit, we remark that in this case where we have exploited the scale invariance

$$\theta(h) = \rho^- \int_{\tilde{h}}^{h} \frac{k_1 k_2}{(k_1^2 - k_2^2)\sqrt{u_1 u_2}}\, \mathrm{d}h,$$

since we now take $\beta_1 = \beta_2 = 1$. (θ is not scale invariant.)

REFERENCES

Athanassoulis, G. A. & Belibassakis, K. A. 1999 A consistent coupled-mode theory for the propagation of small-amplitude water waves over variable bathymetry regions. *J. Fluid Mech.* **389**, 275–301.

Barthélemy, E., Kabbaj, A. & Germain, J.-P. 2000 Long surface wave scattered by a step in a two-layer fluid. *Fluid Dyn. Res.* **26**, 235–255.

Berkhoff, J. C. W. 1973 Computation of combined refraction-diffraction. *Proc. 13th Conf. on Coastal Engng., July 1972, Vancouver, Canada*, vol. 2, pp. 471–490. ASCE.

Berkhoff, J. C. W. 1976 Mathematical models for simple harmonic linear waves. Wave diffraction and refraction. *Delft Hydr. Rep.* W 154-IV.

Cadby, J. R. & Linton, C. M. 2000 Three-dimensional water-wave scattering in two-layer fluids. *J. Fluid Mech.* **423**, 155–173.

Chamberlain, P. G. & Porter, D. 1995 The modified mild-slope equation. *J. Fluid Mech.* **291**, 393–407.

https://doi.org/10.1017/S0022112004002356 Published online by Cambridge University Press

Chen, Y. & Liu, P. L.-F. 1996 On interfacial waves over random topography. *Wave Motion* **24**, 169–184.

Kelly, R. E. 1969 Wave diffraction in a two-fluid system. *J. Fluid Mech.* **36**, 65–73.

Lamb, H. 1932 *Hydrodynamics*. Cambridge University Press.

Lambert, J. D. 1992 *Numerical methods for Ordinary Differential Systems*. Wiley.

Linton, C. M. & Cadby, J. R. 2002 Scattering of oblique waves in a two-layer fluid. *J. Fluid Mech.* **461**, 343–364.

Linton, C. M. & Cadby, J. R. 2003 Trapped modes in a two-layer fluid. *J. Fluid Mech.* **481**, 215–234.

Linton, C. M. & McIver, M. 1995 The interaction of waves with horizontal cylinders in two-layer fluids. *J. Fluid Mech.* **304**, 213–229.

Llewellyn Smith, S. G. & Young, W. R. 2003 Tidal conversion at a very steep ridge. *J. Fluid Mech.* **495**, 175–191.

Luke, J. C. 1967 A variational principle for a fluid with a free surface. *J. Fluid Mech.* **27**, 395–397.

Lynett, J. L. & Liu, P. L.-F. 2002 A two-dimensional, depth integrated model for internal wave propagation over variable bathymetry. *Wave Motion* **36**, 221–240.

Miles, J. 1967 Surface-wave scattering matrix for a shelf. *J. Fluid Mech.* **28**, 755–767.

Porter, D. & Staziker, D. J. 1995 Extensions of the mild slope equation. *J. Fluid Mech.* **300**, 367–382.

Porter, R. & Porter, D. 2001 Interaction of water waves with three-dimensional periodic topography. *J. Fluid Mech.* **434**, 301–335.

Porter, D. 2003 The mild-slope equations. *J. Fluid Mech.* **494**, 51–63.

Porter, R. & Porter, D. 2003 Scattered and free waves over periodic beds. *J. Fluid Mech.* **483**, 129–163.

Silva, R., Salles, P & Palacio, A. 2002 Linear waves propagating over a rapidly varying porous bed. *Coast. Eng.* **44**, 239–260.

Smith, R. & Sprinks, T. 1975 Scattering of surface waves by a conical island. *J. Fluid Mech.* **72**, 373–384.

Wehausen, J. N. & Laitone, E. V. 1960 Surface waves. *Handbuch der Physik*, vol. IX. Springer.

https://doi.org/10.1017/S0022112004002356 Published online by Cambridge University Press